AIMS Mathematics, 11(1): 2595–2612.
DOI:10.3934/math.2026105
Received: 14 November 2025
Revised: 08 January 2026
Accepted: 13 January 2026
Published: 27 January 2026

https://www.aimspress.com/journal/Math

Research article

Amplitude equation for the Hopf bifurcation of a reaction-diffusion predator-prey system incorporating time delay

Ping Li[1], Haisong Cao[1], Can Chen[2] and Jianfeng Jiao[2,*]

[1] School of Mathematics and Statistics, North China University of Water Resources and Electric Power, Zhengzhou 450046, China

[2] Department of Mathematics, Zhengzhou University of Aeronautics, Zhengzhou 450046, China

* **Correspondence:** Email: jfjiaomath@zua.edu.cn.

Abstract: Modeling the interactions between prey and predators has become an important method to reveal their evolutionary patterns. This paper investigated a predator-prey model incorporating Holling II functional response, considering the dynamic effects of time delay and cross-diffusion on the model. First, the existence and local stability of a positive equilibrium were proven without time delay and diffusion. Next, we selected time delay as the bifurcation parameter to study the existence of Hopf bifurcation, and determined the critical value for Hopf bifurcation. Furthermore, by utilizing multi-scale analysis, the amplitude equation was derived, thereby obtaining the direction of Hopf bifurcation and the stability of bifurcation periodic solutions. Our results show that changes in time delay or diffusion parameters can lead to periodic oscillatory solutions in time and space, corresponding to supercritical (subcritical) Hopf bifurcation, and Turing instability. Finally, the theoretical results were validated through numerical simulations.

Keywords: predator-prey model; delay; diffusion; Hopf bifurcation; amplitude equation
Mathematics Subject Classification: 54H20, 35B32, 37C75

1. Introduction

As is well known, the relationships between species are complex and diverse, including predation, parasitism, competition, and mutualistic symbiosis, which together constitute a rich and colorful ecosystem. The predator-prey model is an important ecosystem model that describes the dynamic interactions between two organisms. This has long been an important topic in ecology and mathematics, and it has already obtained many research results [1–3].

The first predator-prey model in ecological history was proposed by Lotka-Volterra (L-V) [4, 5], which laid the foundation for subsequent research. In the classic L-V model, the predation term is

linear, which means that the predation rate increases linearly with prey density, and there is no limit to the number of prey that each predator can kill, which is clearly unrealistic. In fact, the amount of food that a predator can eat in a day is limited. When the prey is very abundant, it will not hunt again while being full. In order to enhance the realism of the model, Holling proposed three main types of functional responses, including Holling I, Holling II, and Holling III [6, 7], and then used functional responses to replace the overly simplified predation term in the L-V model, greatly improving the model's realism and predictive ability. Therefore, inspired by the above ideas and reference [8], this paper considers a predator-prey model with Holling II functional response

$$\begin{cases} \dfrac{du}{dt} = u(1-u) - \dfrac{uv}{u+\alpha}, \\ \dfrac{dv}{dt} = \dfrac{ruv}{u+\alpha} - \sigma v, \end{cases} \tag{1.1}$$

where u and v is the density of prey and predator population at the time t. $u(1-u)$ describes the self growth of prey in the absence of predators. Predation of prey species by predators is quantified by a Holling type-II functional response, which is given by $\frac{uv}{u+\alpha}$, where α represents the half saturation rate. r is the conversion efficiency of predators, and the value of r is between 0 and 1 based on ecological reasons. σ represents the mortality rate of predators.

Due to the interactions between populations in ecosystems, time delay is a common phenomenon. For example, pregnancy delay refers to the time it takes for predators to catch prey and produce the next generation [9]. On the other hand, a delay caused by the regrowth of consumed resources (such as plant biomass) is called resource regeneration delay, while Poisoning delay refers to the delay in poisoning of animals after consuming toxic food, as they will wait for a period of time before symptoms appear [10]. At present, multiple papers have studied the impact of delay on population dynamic behavior. For example, delay can trigger Hopf bifurcation by adjusting interspecific or intraspecific feedback, thereby disrupting the stability of the system equilibrium and generating periodic oscillation behavior [11–13]. In this paper, we consider that the physiological characteristics of a species, such as the length of pregnancy, may themselves determine whether its population will experience a "boom-bust" cycle. This has important implications for conservation biology and pest management, that is, we need to pay attention to those key life cycle parameters that may themselves be sources of risk for population instability. Based on the above viewpoint, a more reasonable predator-prey model with delay is obtained as

$$\begin{cases} \dfrac{du}{dt} = u(1-u) - \dfrac{uv}{u+\alpha}, \\ \dfrac{dv}{dt} = \dfrac{ru(t-\tau)v}{u(t-\tau)+\alpha} - \sigma v, \end{cases} \tag{1.2}$$

where τ represents the pregnancy delay.

In nature, everything not only evolves in time, but also undergoes non-homogeneous evolution in space. For predation models, considering the discrete distribution of population habitats in ecosystems and the interactions between populations in different habitats, we know that the survival behavior of populations involves self-diffusion and cross-diffusion. Self-diffusion is mainly used to describe the random walks of individuals within their habitat. However, prey tends to stay away from predators in order to avoid capture, which causes changes in the concentration levels of prey [14, 15]. Meanwhile, the movement of predators is also influenced by the concentration gradient of prey at the same location.

This phenomenon is usually described by cross-diffusion [16, 17]. In addition, the dynamic study of spatial models has always been one of the main topics in the field of biological mathematics [18–20]. Therefore, it is significant to study the impact of self and cross-diffusion on the interactions between species, and finally establish the following delayed reaction-diffusion system

$$\begin{cases} \dfrac{\partial u(x,t)}{dt} = d_{11}\Delta u(x,t) + d_{12}\Delta v(x,t) + u(x,t)(1-u(x,t)) - \dfrac{u(x,t)v(x,t)}{u(x,t)+\alpha}, x \in \Omega,\ t > 0, \\ \dfrac{\partial v(x,t)}{dt} = d_{21}\Delta u(x,t) + d_{22}\Delta v(x,t) + \dfrac{ru(x,t-\tau)v(x,t)}{u(x,t-\tau)+\alpha} - \sigma v(x,t), x \in \Omega,\ t > 0, \\ \dfrac{\partial u(x,t)}{\partial n} = \dfrac{\partial v(x,t)}{\partial n} = 0, x \in \partial\Omega,\ t \geq 0, \\ u(x,t) = u_0(x,t) \geq 0, \quad v(x,t) = v_0(x,t) \geq 0, (x,t) \in \overline{\Omega} \times [-\tau, 0], \end{cases} \tag{1.3}$$

where d_{11} and d_{22} are the self-diffusion coefficients of prey and predator, respectively, which are nonnegative and describe the random movement of species. d_{12} and d_{21} are the cross-diffusion coefficients of predators and prey, respectively, which are positive and negative values or zero. According to [16, 21], we assume $d_{11}d_{22} - d_{12}d_{21} > 0$. Δ is the Laplace operator, and $\Omega = (0, \pi)$ is a smooth and bounded domain. The homogeneous Neumann boundary condition $\frac{\partial u(x,t)}{\partial n} = \frac{\partial v(x,t)}{\partial n} = 0$ means that no species enter or leave this area, where n is the outward unit normal vector to the boundary $\partial\Omega$, and $u_0(x,t)$ and $v_0(x,t)$ respectively represent the initial conditions.

The main contributions of this study are summarized as follows: in the model construction, we considered the time delay required for predators to capture prey and generate the next generation, and discussed the critical conditions for Hopf bifurcation. Furthermore, using multi-scale analysis, we derived the amplitude equation of the system when Hopf bifurcation occurs near positive equilibrium, revealing rich spatiotemporal pattern dynamics. The multi-scale analysis is the core method for solving weakly nonlinear amplitude equations. Its fundamental idea is that, given the characteristic that solutions of weakly nonlinear systems evolve at different rates across different time scales, multiple independent time variables are introduced to decompose the original equations into different scales and solve them step by step, thereby obtaining high-precision amplitude evolution equations. This enables precise analytical insights into the coupling effects of Holling II functional response, time delay, and cross-diffusion on population dynamics across different scales. Finally, numerical analysis shows that both self-diffusion and cross-diffusion can induce Turing instability. Based on the above results, we will improve the system performance by adjusting the time delay and diffusion coefficient, in order to gain a deeper understanding of their impact on the dynamics of the ecosystem.

The subsequent sections are organized as follows. First, the existence and stability of equilibria and the conditions to ascertain the local stability of the Hopf bifurcation are conducted in Section 2. Subsequently, we use multi-scale analysis to separate the delayed reaction-diffusion system on the time scale, simplify the complex nonlinear system to a topologically equivalent amplitude equation, and analyze the dynamic behavior of the amplitude equation in Section 3. To validate the obtained results, in Section 4, numerical simulation are carried out. Some conclusions are given to conclude our work in Section 5.

2. Local stability and Hopf bifurcation

2.1. The existence of equilibria

In this subsection, we mainly analyze the existence of the equilibria for system (1.1). It is easy to know that the trivial equilibrium $E_0(0,0)$ and semi-trivial equilibrium $E_1(1,0)$ of system (1.1) always exist. From the perspective of species diversity, the coexistence of two species is very meaningful. Therefore, we assume that $E^*(u^*, v^*)$ is the coexistence equilibrium of system (1.1) with $u^* = \frac{\sigma\alpha}{r-\sigma}$ and $v^* = \frac{\alpha r(r-\sigma-\sigma\alpha)}{(r-\sigma)^2}$. Importantly, if $H_0 : r > \sigma(\alpha+1)$ holds, the system (1.1) has a unique positive coexistence equilibrium $E^*(u^*, v^*)$.

2.2. Local stability of positive equilibrium E^* and Hopf bifurcation

Under the condition that H_0 holds, we only discuss the local stability of positive coexistence equilibrium E^* and further study the existence of Hopf bifurcation by analyzing the characteristic equation of the system (1.3). Subsequently, the derivation process of the characteristic equation is as follows: First, introducing small perturbations near E^*, that is $u(x,t) = u^* + \tilde{u}(x,t)$ and $v(x,t) = v^* + \tilde{v}(x,t)$, where $\tilde{u}(x,t)$ and $\tilde{v}(x,t)$ are small perturbation amounts. Substituting $\tilde{u}(x,t)$ and $\tilde{v}(x,t)$ into the system (1.3), then the linearized system of (1.3) can be written as

$$\begin{cases} \dfrac{\partial\tilde{u}(x,t)}{\partial t} = d_{11}\Delta\tilde{u}(x,t) + d_{12}\Delta\tilde{v}(x,t) + a_{11}\tilde{u}(x,t) - a_{12}\tilde{v}(x,t), \\ \dfrac{\partial\tilde{v}(x,t)}{\partial t} = d_{21}\Delta\tilde{u}(x,t) + d_{22}\Delta\tilde{v}(x,t) + a_{21}\tilde{u}(x,t-\tau), \end{cases} \tag{2.1}$$

where $a_{11} = 1 - 2u^* - \frac{\alpha v^*}{(\alpha+u^*)^2}$, $a_{12} = \frac{u^*}{\alpha+u^*} > 0$, $a_{21} = \frac{r\alpha v^*}{(\alpha+u^*)^2} > 0$.

Assuming $\tilde{u}(x,t) = c_1 e^{\lambda t+ikx}$, $\tilde{v}(x,t) = c_2 e^{\lambda t+ikx}$, where c_1 and c_2 correspond to the amplitude of $\tilde{u}(x,t)$ and $\tilde{v}(x,t)$ near E^* respectively. λ represents the eigenvalue, which determines whether the disturbance increases or decreases over time, and $Re(\lambda) > 0$ indicates instability. k represents wave number ($k = 0, 1, 2, 3, ...$). e^{ikx} represents spatial harmonics. For the time delay term, $\tilde{u}(x, t-\tau) = c_1 e^{\lambda(t-\tau)+ikx} = e^{-\lambda\tau}\tilde{u}(x,t)$.

Next, substituting $\tilde{u}(x,t)$, $\tilde{u}(x,t-\tau)$ and $\tilde{v}(x,t)$ into the linearized Eq (2.1), we obtain the characteristic equation in matrix form

$$\begin{pmatrix} \lambda + d_{11}k^2 - a_{11} & d_{12}k^2 + a_{12} \\ d_{21}k^2 - a_{21}e^{-\lambda\tau} & \lambda + d_{22}k^2 \end{pmatrix}\begin{pmatrix} c_1 \\ c_2 \end{pmatrix} = 0.$$

To ensure the existence of non-zero solutions, the determinant of the matrix is zero. Thus, the characteristic equation is

$$\lambda^2 + a_k\lambda + b_k + c_k e^{-\lambda\tau} = 0, \tag{2.2}$$

where $a_k = d_{11}k^2 + d_{22}k^2 - a_{11}$, $b_k = (d_{11}d_{22} - d_{12}d_{21})k^4 - (a_{12}d_{21} + a_{11}d_{22})k^2$, $c_k = a_{21}d_{12}k^2 + a_{12}a_{21} > 0$.

Finally, analyzing the characteristic Eq (2.2) when $\tau = 0$ and $\tau > 0$, the local stability of positive equilibrium E^* and the existence of Hopf bifurcation are studied as follows.

2.2.1. The local stability of ordinary differential equation (ODE) ($\tau = 0, k = 0$)

When $\tau = 0, k = 0$, the characteristic Eq (2.2) becomes

$$\lambda^2 + a_0\lambda + b_0 + c_0 = 0, \tag{2.3}$$

where $a_0 = -a_{11}, c_0 = a_{12}a_{21} > 0$.

If $H_1 : a_0 > 0, b_0 + c_0 > 0$ holds, then all roots of the Eq (2.3) have negative real parts, which means the positive equilibrium E^* is locally asymptotically stable. Summarizing the above analysis, we can obtain the local stability of equilibrium E^* of the ordinary differential system (1.1).

Lemma 2.1. *Assuming that the existence condition H_0 of the positive equilibrium E^* is satisfied. If H_1 holds, then the positive equilibrium E^* is locally asymptotically stable.*

2.2.2. The local stability of reaction-diffusion equation in E^* ($\tau = 0, k > 0$)

When $\tau = 0, k > 0$, the characteristic Eq (2.2) can be written as

$$\lambda^2 + a_k\lambda + b_k + c_k = 0. \tag{2.4}$$

Under the condition that ODE is stable, $a_k > a_0 > 0$ is obviously true, so all roots of the Eq (2.4) have negative real parts if and only if $b_k + c_k > 0$ for all k. According to the expression of b_k, c_k and donating $m = k^2$, we get

$$b_k + c_k = (d_{11}d_{22} - d_{12}d_{21})k^4 + (a_{21}d_{12} - a_{12}d_{21} - a_{11}d_{22})k^2 - a_{12}a_{21} = \rho_1 m^2 + \rho_2 m + \rho_3,$$

where $\rho_1 = d_{11}d_{22} - d_{12}d_{21} > 0, \rho_2 = a_{21}d_{12} - a_{12}d_{21} - a_{11}d_{22}, \rho_3 = a_{12}a_{21} > 0, \Delta_0 = \rho_2^2 - 4\rho_1\rho_3$. Further, we give two assumptions: $H_2 : \Delta_0 < 0$; $H_3 : \Delta_0 > 0, \rho_2 > 0$. Then, we can get the following results about the local stability of equilibrium E^* of the reaction-diffusion system.

Lemma 2.2. *Assuming that the existence condition H_0 and the stability condition H_1 of the positive equilibrium E^* are satisfied, if H_2 or H_3 holds, then $b_k + c_k > 0$ for all k. Thus, the positive equilibrium E^* is locally asymptotically stable.*

Proof. We know that $a_k > a_0 > 0$ when H_1 holds, and $\rho_3 > 0$ is obviously true. If H_2 or H_3 holds, then we can obtain $b_k + c_k > 0$ for all k, and at this time, all roots of Eq (2.4) have negative real parts. Thus, the positive equilibrium E^* is locally asymptotically stable. □

Theorem 2.1. *Assuming that the existence condition H_0 and the stability condition H_1 of the positive equilibrium E^* are satisfied, if $\Delta_0 > 0$, $\rho_2 < 0$, and $k \in (\sqrt{m_1}, \sqrt{m_2})$, where k is a nonnegative integer, $m_1 = \frac{-\rho_2 - \sqrt{\Delta_0}}{2\rho_1}, m_2 = \frac{-\rho_2 + \sqrt{\Delta_0}}{2\rho_1}$, then $b_k + c_k < 0$, that is, Eq* (2.4) *has two roots with opposite signs, meaning the system* (1.3) *presents Turing instability.*

Proof. We know that $\rho_1 > 0$ and $\rho_3 > 0$ are obviously true. If $\Delta_0 > 0$ and $\rho_2 < 0$ hold, then $b_k + c_k = 0$ has two positive roots m_1 and m_2, where $m_1 = \frac{-\rho_2 - \sqrt{\Delta_0}}{2\rho_1}, m_2 = \frac{-\rho_2 + \sqrt{\Delta_0}}{2\rho_1}$. Further, when $k \in (\sqrt{m_1}, \sqrt{m_2})$, $b_k + c_k < 0$, that is, Eq (2.4) has two roots with opposite signs, thus the system (1.3) presents Turing instability. Further, we can get the critical wavenumber $k_c^2 = -\frac{\rho_2}{2\rho_1}$ and then the characteristic wavelength $\lambda_{k_c} = \frac{2\pi}{k_c} = 2\pi\sqrt{-\frac{2\rho_1}{\rho_2}}$. □

2.2.3. The local stability of time-delay reaction-diffusion system in E^* ($\tau > 0$)

Assuming that $\lambda_k = \pm i\omega_k(\omega_k > 0)$ is a pair of purely imaginary roots of Eq (2.2) and dividing the real and imaginary parts, we get

$$\begin{cases} \cos(\omega_k\tau) = \dfrac{\omega_k^2 - b_k}{c_k}, \\ \sin(\omega_k\tau) = \dfrac{a_k\omega_k}{c_k}. \end{cases} \tag{2.5}$$

Taking the sum of squares of the corresponding sides of Eq (2.5), we obtain

$$\omega_k^4 + (a_k^2 - 2b_k)\omega_k^2 + b_k^2 - c_k^2 = 0. \tag{2.6}$$

Denoting $z_k = \omega_k^2$, Eq (2.6) can be written as

$$h(z_k) = z_k^2 + (a_k^2 - 2b_k)z_k + b_k^2 - c_k^2 = 0, \tag{2.7}$$

where $a_k^2 - 2b_k = (2d_{12}d_{21} + d_{22}^2)k^4 + (d_{11}k^2 - a_{11})^2 + 2a_{12}d_{21}k^2 > 0$, $\Delta_{h(z_k)} = (a_k^2 - 2b_k)^2 - 4(b_k^2 - c_k^2)$.

When $\Delta_{h(z_k)} < 0$, Eq (2.7) has no positive real root. On the contrary, when $\Delta_{h(z_k)} > 0$, we assume that z_k^1 and z_k^2 are two roots of Eq (2.7). Since $z_k^1 + z_k^2 = -(a_k^2 - 2b_k) < 0$, Eq (2.7) has only a positive root if and only if $z_k^1 z_k^2 = (b_k + c_k)(b_k - c_k) < 0$. Further, under the condition that H_2 or H_3 holds, $b_k + c_k > 0$, thereby Eq (2.7) has only a positive root if and only if $b_k - c_k < 0$, which means Eq (2.2) has a pair of pure imaginary roots. According to the expression of b_k and c_k, and donating $m = k^2$, we get

$$b_k - c_k = (d_{11}d_{22} - d_{12}d_{21})k^4 + (-a_{12}d_{21} - a_{21}d_{12} - a_{11}d_{22})k^2 - a_{12}a_{21} = \rho_1 m^2 + \rho_4 m + \rho_5, \tag{2.8}$$

where $\rho_1 = d_{11}d_{22} - d_{12}d_{21} > 0, \rho_4 = -a_{12}d_{21} - a_{21}d_{12} - a_{11}d_{22} < \rho_2, \rho_5 = -a_{12}a_{21} < 0 < \rho_3$, $\Delta_1 = \rho_4^2 - 4\rho_1\rho_5 > 0$.

From Eq (2.8), it is easy to know that when $k \in [0, \sqrt{m_3}), (m_3 = \frac{-\rho_4 + \sqrt{\Delta_1}}{2\rho_1})$, then $b_k - c_k < 0$. Based on the above analysis, we obtain the following lemma.

Lemma 2.3. *Assuming that the existence condition H_0 and the stability condition H_1 of the positive equilibrium E^* are satisfied, and H_2 or H_3 holds, when $k \in [0, \sqrt{m_3})$, where k is a nonnegative integer and $m_3 = \frac{-\rho_4 + \sqrt{\Delta_1}}{2\rho_1}$, then $b_k + c_k > 0$ and $b_k - c_k < 0$ are established simultaneously.*

According to Lemma 2.3, we can obtain a positive root ω_k of Eq (2.6), which is written as

$$\omega_k = \sqrt{\frac{2b_k - a_k^2 + \sqrt{a_k^4 - 4a_k^2 b_k + 4c_k^2}}{2}}. \tag{2.9}$$

The associated critical value of delay is

$$\tau_k^{(j)} = \frac{1}{\omega_k}\Big[2j\pi + \arccos\left(\frac{\omega_k^2 - b_k}{c_k}\right)\Big], k \in [0, \sqrt{m_3}), j = 0, 1, 2, 3.... \tag{2.10}$$

Denoting $\tau_c = \min\left\{\tau_k^{(j)}\right\}$, and $\lambda_k(\tau) = \alpha_k(\tau) \pm i\beta_k(\tau)$ is a pair of eigenvalues of Eq (2.2), which satisfies $\alpha_k(\tau_c) = 0, \beta_k(\tau_c) = \omega_k$. Next, consider the transversal condition for the occurrence of Hopf bifurcation. First, differentiating both sides of Eq (2.2) with respect to τ, we get

$$\left(\frac{d\lambda_k}{d\tau}\right)^{-1} = \frac{(2\lambda_k + a_k)e^{\lambda_k\tau}}{c_k\lambda_k} - \frac{\tau}{\lambda_k}. \tag{2.11}$$

Second, taking the real part of Eq (2.11), we have

$$Re\left(\frac{d\lambda_k}{d\tau}\right)^{-1}_{\tau=\tau_c} = \frac{2\omega_k^2 + a_k^2 - 2b_k}{c_k^2}. \tag{2.12}$$

Finally, according to $a_k^2 - 2b_k = (2d_{12}d_{21} + d_{22}^2)k^4 + (d_{11}k^2 - a_{11})^2 + 2a_{12}d_{21}k^2 > 0$, then $Re\left(\frac{d\lambda_k}{d\tau}\right)^{-1}_{\tau=\tau_c} > 0$, which means that the transversal condition is satisfied. Using the Hopf bifurcation theory, we can obtain the following theorem.

Theorem 2.2. *Assuming that the existence condition H_0 and the stability condition H_1 of the positive equilibrium E^*, H_2 or H_3 holds, $k \in [0, \sqrt{m_3})$, and k is a nonnegative integer.*

(1) *When $\tau < \tau_c$, the positive equilibrium E^* is locally asymptotically stable.*
(2) *When $\tau > \tau_c$, the positive equilibrium E^* is unstable.*
(3) *When $\tau = \tau_c$, the system* (1.3) *undergoes Hopf bifurcation.*

3. Amplitude equation of Hopf bifurcation

In this section, we consider extending the multi-scale analysis to the predator-prey reaction-diffusion systems with time delay and derive the amplitude equation of the Hopf bifurcation at $E^*(u^*, v^*)$. By making the time scale transformation ($t \to \frac{t}{\tau}$) for system (1.3), we can get

$$\begin{cases} \dfrac{\partial u(x,t)}{\partial t} = \tau\Big[d_{11}\Delta u(x,t) + d_{12}\Delta v(x,t) + u(x,t)(1-u(x,t)) - \dfrac{u(x,t)v(x,t)}{u(x,t)+\alpha}\Big], \\ \dfrac{\partial v(x,t)}{\partial t} = \tau\Big[d_{21}\Delta u(x,t) + d_{22}\Delta v(x,t) + \dfrac{ru(x,t-1)v(x,t)}{u(x,t-1)+\alpha} - \sigma v(x,t)\Big]. \end{cases} \tag{3.1}$$

After Taylor expansion of Eq (3.1) at equilibrium E^*, we can obtain

$$\begin{cases} \dfrac{\partial u(x,t)}{\partial t} =\tau\Big[d_{11}\Delta u(x,t) + d_{12}\Delta v(x,t) + a_{11}u(x,t) - a_{12}v(x,t) \\ \qquad\qquad - p_1u^2(x,t) - p_2u(x,t)v(x,t) + O(u^3(x,t))\Big], \\ \dfrac{\partial v(x,t)}{\partial t} =\tau\Big[d_{21}\Delta u(x,t) + d_{22}\Delta v(x,t) + a_{21}u(x,t-1) \\ \qquad\qquad - q_1u^2(x,t-1) + q_2u(x,t-1)v(x,t) + O(u^3(x,t-1))\Big], \end{cases} \tag{3.2}$$

where $p_1 = 1 - \frac{\alpha v^*}{(\alpha+u^*)^3}$, $p_2 = \frac{\alpha}{(\alpha+u^*)^2} > 0$, $q_1 = \frac{r\alpha v^*}{(\alpha+u^*)^3} > 0$, $q_2 = \frac{r\alpha}{(\alpha+u^*)^2} > 0$.

The multi-scale analysis can systematically separate fast and slow variables by introducing different time variables, and accurately capturing system evolution. In addition, Taylor expansion based on the MTS idea can eliminate long-term terms and ensure solution consistency. Specifically, the basic steps of the computational process are as follows:

Step 1. Preparation

Assume that Eq (3.2) has the following form of solution:

$$\begin{pmatrix} u(x,t) \\ v(x,t) \end{pmatrix} = \begin{pmatrix} u(x,T_0,T_1,T_2,...) \\ v(x,T_0,T_1,T_2,...) \end{pmatrix} = \sum_{m=1}^{\infty} \varepsilon^m \begin{pmatrix} u_m(x,T_0,T_1,T_2,...) \\ v_m(x,T_0,T_1,T_2,...) \end{pmatrix}, \tag{3.3}$$

where $T_g = \varepsilon^g t$ $(g = 0, 1, 2, 3, ...)$ is the scale transformation on time direction. Then, differentiating $T_g = \varepsilon^g t$ with respect to time t by the chain rule, we have $\frac{\partial}{\partial t} = \frac{\partial}{\partial T_0} + \varepsilon \frac{\partial}{\partial T_1} + \varepsilon^2 \frac{\partial}{\partial T_2} + ... = D_0 + \varepsilon D_1 + \varepsilon^2 D_2 + ...$, where $D_g = \frac{\partial}{\partial T_g}$, $g = 0, 1, 2, ...$ Furthermore, we can obtain the following expression:

$$\begin{aligned}
\frac{\partial}{\partial t}\begin{pmatrix} u(x,t) \\ v(x,t) \end{pmatrix} &= \varepsilon D_0 \begin{pmatrix} u_1(x, T_0, T_1, T_2, ...) \\ v_1(x, T_0, T_1, T_2, ...) \end{pmatrix} + \varepsilon^2 \Big[D_0 \begin{pmatrix} u_2(x, T_0, T_1, T_2, ...) \\ v_2(x, T_0, T_1, T_2, ...) \end{pmatrix} \\
&\quad + D_1 \begin{pmatrix} u_1(x, T_0, T_1, T_2, ...) \\ v_1(x, T_0, T_1, T_2, ...) \end{pmatrix} \Big] + \varepsilon^3 \Big[D_0 \begin{pmatrix} u_3(x, T_0, T_1, T_2, ...) \\ v_3(x, T_0, T_1, T_2, ...) \end{pmatrix} \\
&\quad + D_1 \begin{pmatrix} u_2(x, T_0, T_1, T_2, ...) \\ v_2(x, T_0, T_1, T_2, ...) \end{pmatrix} + D_2 \begin{pmatrix} u_1(x, T_0, T_1, T_2, ...) \\ v_1(x, T_0, T_1, T_2, ...) \end{pmatrix} \Big] + ..., \\
\begin{pmatrix} \Delta u(x,t) \\ \Delta v(x,t) \end{pmatrix} &= \varepsilon \begin{pmatrix} \Delta u_1(x, T_0, T_1, T_2, ...) \\ \Delta v_1(x, T_0, T_1, T_2, ...) \end{pmatrix} + \varepsilon^2 \begin{pmatrix} \Delta u_2(x, T_0, T_1, T_2, ...) \\ \Delta v_2(x, T_0, T_1, T_2, ...) \end{pmatrix} \\
&\quad + \varepsilon^3 \begin{pmatrix} \Delta u_3(x, T_0, T_1, T_2, ...) \\ \Delta v_3(x, T_0, T_1, T_2, ...) \end{pmatrix} + ..., \\
v(x, t-1) &= \varepsilon v_{1,1} + \varepsilon^2 (v_{2,1} - D_1 v_{1,1}) + \varepsilon^3 (v_{3,1} - D_1 v_{2,1} - D_2 v_{1,1}) + ...
\end{aligned} \tag{3.4}$$

Please see Appendix for the calculation process of $v(x, t-1)$. Next, take the time delay τ as the bifurcation parameter, and further expand it into a power series with a small quantity ε near the critical value τ_c, that is, $\tau = \tau_c + \varepsilon\tau_1 + \varepsilon^2\tau_2 + ...$ Finally, substitute τ and Eqs (3.3) and (3.4) into Eq (3.2), and then compare the orders of ε, and the following results are obtained:

Step 2. The coefficient expression of ε, ε^2 and ε^3

$$O(\varepsilon): \begin{cases} D_0 u_1 - \tau_c(d_{11}\Delta u_1 + d_{12}\Delta v_1 + a_{11}u_1 - a_{12}v_1) = 0, \\ D_0 v_1 - \tau_c(d_{21}\Delta u_1 + d_{22}\Delta v_1 + a_{21}u_{1,1}) = 0. \end{cases} \tag{3.5}$$

$$O(\varepsilon^2): \begin{cases} D_0 u_2 - \tau_c(d_{11}\Delta u_2 + d_{12}\Delta v_2 + a_{11}u_2 - a_{12}v_2) \\ = -D_1 u_1 - \tau_c(p_1 u_1^2 + p_2 u_1 v_1) + \tau_1(d_{11}\Delta u_1 + d_{12}\Delta v_1 + a_{11}u_1 - a_{12}v_1), \\ D_0 v_2 - \tau_c(d_{21}\Delta u_2 + d_{22}\Delta v_2 + a_{21}u_{2,1}) \\ = -D_1 v_1 + \tau_c(-q_1 u_{1,1}^2 + q_2 u_{1,1} v_1 - a_{21} D_1 u_{1,1}) + \tau_1(d_{21}\Delta u_1 + d_{22}\Delta v_1 + a_{21}u_{1,1}). \end{cases} \tag{3.6}$$

$$O(\varepsilon^3): \begin{cases} D_0 u_3 - \tau_c(d_{11}\Delta u_3 + d_{12}\Delta v_3 + a_{11}u_3 - a_{12}v_3) \\ = -D_1 u_2 - D_2 u_1 - \tau_c(2p_1 u_1 u_2 + p_2 u_1 v_2 + p_2 u_2 v_1) \\ \quad + \tau_1(d_{11}\Delta u_2 + d_{12}\Delta v_2 + a_{11}u_2 - a_{12}v_2 - p_1 u_1^2 - p_2 u_1 v_1), \\ D_0 v_3 - \tau_c(d_{21}\Delta u_3 + d_{22}\Delta v_3 + a_{21}u_{3,1}) \\ = -D_1 v_2 - D_2 v_1 + \tau_c\Big(- 2q_1 u_{1,1}(u_{2,1} - D_1 u_{1,1}) + q_2 v_1 (u_{2,1} - D_1 u_{1,1}) \\ \quad + q_2 v_2 u_{1,1} - a_{21}(D_1 u_{2,1} + D_2 u_{1,1})\Big) + \tau_1\big(- q_1 u_{1,1}^2 + q_2 u_{1,1} v_1 \\ \quad + d_{21}\Delta u_2 + d_{22}\Delta v_2 + a_{21}u_{2,1} - a_{21} D_1 u_{1,1}). \end{cases} \tag{3.7}$$

Step 3. The solution of u_1, v_1, u_2, v_2 and the Fredholm alternative condition

(1) Assuming Eq (3.5) has the following form of solution

$$\begin{pmatrix} u_1(x, T_0, T_1, T_2, ...) \\ v_1(x, T_0, T_1, T_2, ...) \end{pmatrix} = G e^{i\omega_k \tau_c T_0} \boldsymbol{h} \cos kx + \bar{G} e^{-i\omega_k \tau_c T_0} \bar{\boldsymbol{h}} \cos kx, \tag{3.8}$$

where $G = G(T_1, T_2, ...)$ is the complex amplitude. $\cos(kx)$ is the spatial characteristic function. $\boldsymbol{h} = (h_{11}, h_{12})^{\mathrm{T}}$ is a vector that needs to be determined. Next, substituting $u_{1,1} = G e^{i\omega_k \tau_c (T_0 - 1)} h_{11} \cos kx +$

$\bar{G}e^{-i\omega_k\tau_c(T_0-1)}\bar{h}_{11}\cos kx$ and Eq (3.8) into Eq (3.5), and then comparing the coefficients of $Ge^{i\omega_k\tau_c T_0}$, we have $\boldsymbol{h} = (h_{11}, h_{12})^{\mathrm{T}} = (\frac{d_{12}k^2+a_{12}}{a_{11}-i\omega_k-d_{11}k^2}, 1)^{\mathrm{T}}$. Further, we obtain the linear matrix $C = \tau_c\begin{pmatrix} -d_{11}k^2+a_{11} & -d_{12}k^2-a_{12} \\ -d_{21}k^2+a_{21}e^{-\lambda} & -d_{22}k^2 \end{pmatrix}$ from Eq (3.5). Note that $\boldsymbol{h}^* = (h_{21}, h_{22})^{\mathrm{T}}$ is the eigenvectors corresponding to eigenvalue $\lambda = -i\omega_k\tau_c$ of adjoint matrix of C. To satisfy $\langle \boldsymbol{h}^*, \boldsymbol{h}\rangle = (\boldsymbol{h}^*)^{\mathrm{T}}\boldsymbol{h} = 1$, we select $\boldsymbol{h}^* = (h_{21}, h_{22})^{\mathrm{T}} = (\frac{d_{12}k^2+a_{12}}{d_{22}k^2-i\omega_k}, 1)^{\mathrm{T}}$, where $l = (1 + \frac{(d_{12}k^2+a_{12})^2}{(d_{22}k^2-i\omega_k)(a_{11}-i\omega_k-d_{11}k^2)})^{-1}$.

Next, substituting $u_{1,1} = Ge^{i\omega_k\tau_c(T_0-1)}h_{11}\cos kx + \bar{G}e^{-i\omega_k\tau_c(T_0-1)}\bar{h}_{11}\cos kx$ and Eq (3.8) into the right (3.6), and denoting the coefficient vector of term $e^{i\omega_k\tau_c T_0}$ as $\boldsymbol{m}_1$, from the Fredholm alternative condition $\langle \boldsymbol{h}^*, \boldsymbol{m}_1\rangle = 0$, we have the expression of $\frac{\partial G}{\partial T_1}$ as

$$\frac{\partial G}{\partial T_1} = M\tau_1 G,$$

where $M = \frac{1}{\bar{h}_{21}h_{11}+\bar{h}_{22}h_{12}+a_{21}\bar{h}_{22}h_{11}\tau_c e^{-i\omega_k\tau_c}}[-(d_{11}\bar{h}_{21}h_{11} + d_{12}\bar{h}_{21}h_{12} + d_{21}\bar{h}_{22}h_{11} + d_{22}\bar{h}_{22}h_{12})k^2 + a_{11}\bar{h}_{21}h_{11} - a_{12}\bar{h}_{21}h_{12} + \bar{h}_{22}h_{11}a_{21}e^{-i\omega_k\tau_c}]$.

(2) Assuming Eq (3.6) has the solution in the following form:

$$\begin{cases} u_2(x, T_0, T_1, T_2, ...) = \sum\limits_{n=0}^{+\infty}(\eta_{0,n}G\bar{G} + \eta_{1,n}G^2e^{2i\omega_k\tau_c T_0} + \bar{\eta}_{1,n}\bar{G}^2e^{-2i\omega_k\tau_c T_0})\cos(nx), \\ v_2(x, T_0, T_1, T_2, ...) = \sum\limits_{n=0}^{+\infty}(\xi_{0,n}G\bar{G} + \xi_{1,n}G^2e^{2i\omega_k\tau_c T_0} + \bar{\xi}_{1,n}\bar{G}^2e^{-2i\omega_k\tau_c T_0})\cos(nx), \end{cases} \tag{3.9}$$

where $\eta_{0,n}, \eta_{1,n}, \xi_{0,n}, \xi_{1,n}$ are parameters that need to be determined. Next, substituting $u_{2,1} = \sum\limits_{n=0}^{+\infty}(\eta_{0,n}G\bar{G}+\eta_{1,n}G^2e^{2i\omega_k\tau_c(T_0-1)}+\bar{\eta}_{1,n}\bar{G}^2e^{-2i\omega_k\tau_c(T_0-1)})\cos(nx)$ (3.8) and (3.9) into (3.6), and then comparing the coefficients of $G\bar{G}$ and $G^2e^{2i\omega_k\tau_c T_0}$, we have

$$\begin{cases} \eta_{0,n} = & -\frac{\kappa_n}{F_0}\Big[-(d_{12}n^2+a_{12})(q_2e^{-i\omega_k\tau_c}(h_{12}\bar{h}_{11}+h_{11}\bar{h}_{12}) - 2q_1h_{11}\bar{h}_{11}) \\ & -(2p_1\bar{h}_{11}h_{11} + p_2h_{12}\bar{h}_{11} + p_2h_{11}\bar{h}_{12})d_{22}n^2\Big], \\ \xi_{0,n} = & \frac{\kappa_n}{F_0}\Big[(-d_{11}n^2+a_{11})(q_2e^{-i\omega_k\tau_c}(h_{12}\bar{h}_{11}+h_{11}\bar{h}_{12}) - 2q_1h_{11}\bar{h}_{11}) \\ & -(2p_1\bar{h}_{11}h_{11} + p_2h_{12}\bar{h}_{11} + p_2h_{11}\bar{h}_{12})(d_{21}n^2-a_{21})\Big], \\ \eta_{1,n} = & -\frac{\kappa_n}{F_1}\Big[(d_{12}n^2+a_{12})(q_2e^{i\omega_k\tau_c}h_{11}h_{12} - q_1e^{-2i\omega_k\tau_c}h_{11}^2) + (p_1h_{11}^2 + p_2h_{11}h_{12})(d_{22}n^2+2i\omega_k)\Big], \\ \xi_{1,n} = & \frac{\kappa_n}{F_1}\Big[(d_{11}n^2+2i\omega_k-a_{11})(q_2e^{i\omega_k\tau_c}h_{11}h_{12} - q_1e^{-2i\omega_k\tau_c}h_{11}^2) \\ & +(p_1h_{11}^2 + p_2h_{11}h_{12})(d_{21}n^2-a_{21}e^{-2i\omega_k\tau_c})\Big], \end{cases}$$

where $\kappa_n = \langle\cos(kx)\cos(kx), \sec(nx)\rangle$, $F_0 = d_{22}n^2(-d_{11}n^2+a_{11}) + (d_{12}n^2+a_{12})(d_{21}n^2-a_{21})$, $F_1 = (d_{11}n^2-a_{11}+2i\omega_k)(d_{22}n^2+2i\omega_k) - (d_{12}n^2+a_{12})(d_{21}n^2-a_{21}e^{-2i\omega_k\tau_c})$.

(3) For Eq (3.7), substituting $u_{1,1}$, $u_{2,1}$ (3.8) and (3.9) into the right side of (3.7), we have the coefficient vector of term $e^{i\omega_k\tau_c T_0}$ denoted as $\boldsymbol{m}_2$. Using the Fredholm alternative condition $\langle \boldsymbol{h}^*, \boldsymbol{m}_2\rangle = 0$, we have the expression of $\frac{\partial G}{\partial T_2}$ as

$$\frac{\partial G}{\partial T_2} = NG^2\bar{G},$$

where $N = -\tau_c\sum_{n=0}^{+\infty}\frac{(\bar{h}_{21}S_{1,n}-\bar{h}_{22}S_{2,n})cos(nx)}{\bar{h}_{21}h_{11}+\bar{h}_{22}h_{12}+\bar{h}_{22}h_{11}q_1\tau_c e^{-i\omega_k\tau_c}}$, with $S_{1,n} = 2p_1(\bar{h}_{11}\eta_{1,n} + h_{11}\eta_{0,n}) + p_2(\bar{h}_{12}\eta_{1,n} + \bar{h}_{11}\zeta_{1,n} + h_{12}\eta_{0,n} + h_{11}\zeta_{0,n})$, $S_{2,n} = q_2(h_{11}\zeta_{0,n} + \bar{h}_{11}\zeta_{1,n}e^{-i\omega_k\tau_c} + \bar{h}_{12}\zeta_{1,n}e^{-2i\omega_k\tau_c}) - 2q_1e^{-i\omega_k\tau_c}(\bar{h}_{11}\eta_{1,n} + h_{11}\eta_{0,n})$.

Denoting $G \to \frac{G}{\varepsilon}$, the normal form of system (1.3) is

$$\dot{G} = M\tau_\varepsilon G + NG^2\bar{G} + ..., \tag{3.10}$$

where $\tau_\varepsilon = \varepsilon\tau_1$. To simplify the analysis, G is expressed in polar coordinates $G = \gamma e^{i\theta}$, where γ represents radial distance, and θ is the phase angle. Then, $G^2\bar{G}$ can be written as $G^2\bar{G} = \gamma^3 e^{i\theta}$. Substituting G, $G^2\bar{G} = \gamma^3 e^{i\theta}$ into (3.10), and neglecting the higher order terms in (3.10), we obtain

$$\begin{cases} \dot{\gamma} = Re(M)\tau_\varepsilon\gamma + Re(N)\gamma^3, \\ \dot{\theta} = Im(M)\tau_\varepsilon + Im(N)\gamma^2. \end{cases}$$

Theorem 3.1. *For $-\infty < \frac{Re(M)\tau_\varepsilon}{Re(N)} < 0$ and τ_ε sufficiently small, then $\dot{\theta} \neq 0$, which means that the existence condition of the periodic solution is satisfied.*

(1) *When $Re(N) < 0$, the Hopf bifurcation is a supercritical bifurcation,meaning that the bifurcation periodic solution is locally asymptotically stable.*
(2) *When $Re(N) > 0$, the Hopf bifurcation is a subcritical bifurcation, meaning that the bifurcation periodic solution is unstable.*

4. Numerical simulation

In this paper, we select $\alpha = 0.3, r = 0.35, \sigma = 0.2$ to verify the correctness of the above theoretical results and replenish the content that cannot be presented in the theoretical calculation.

4.1. Numerical simulation to the stability of equilibria for system (1.1)

In this subsection, we mainly analyze the influence of parameters α, r, and σ on the existence and stability of the equilibria of the system according to bifurcation theory. It can also be observed that α, r, and σ can induce Hopf bifurcation and transcritical bifurcation with increasing bifurcation parameters. Specially, subcritical Hopf bifurcation for α and σ, and r can induce supercritical Hopf bifurcation, which is shown in Figure 1. Further, we select $\alpha = 0.25, 0.3, 1.5$, $r = 0.1, 0.35, 0.4$, and $\sigma = 0.18, 0.2, 0.4$ to observe the changes in the topological structure of system (1.1), as shown in Figure 2(a)–(l). Subsequently, we will take parameter r as an example for specific analysis. In Figure 2(d), the system (1.1), only one stable boundary equilibrium E_1, which means that low predation efficiency leads to the extinction of predators and the proliferation of prey. With the increasing of r, we can observe that there are two equilibria, where the positive equilibrium E^* is stable and the boundary equilibrium E_1 is unstable, as shown in Figure 2(e). Compared to (e), the positive equilibrium E^* becomes unstable, and there is a stable limit cycle around the equilibrium E^* in Figure 2(f), indicating that when r is too high, the predator population can quickly respond to the growth of prey and easily maintain a high density, which may cause the system to tend towards oscillation.

In short, α, r, and σ can affect the topology of system (1.1), and appropriate predation efficiency enables predators to efficiently convert prey into self reproduction, eventually making the system stable.

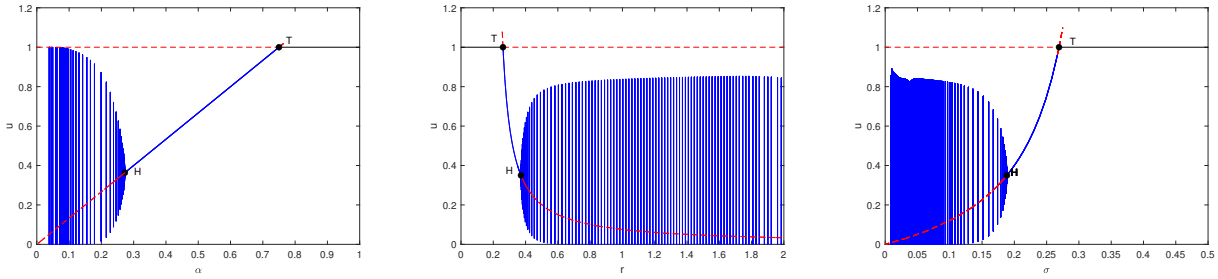

(a) (b) (c)

Figure 1. Bifurcation diagrams of equilibria with different parameters. H represents a Hopf bifurcation. T represents a transcritical bifurcation. The blue and black solid curves represent the stable equilibrium states (limit cycles), while the red dotted curves represent the unstable equilibrium states.

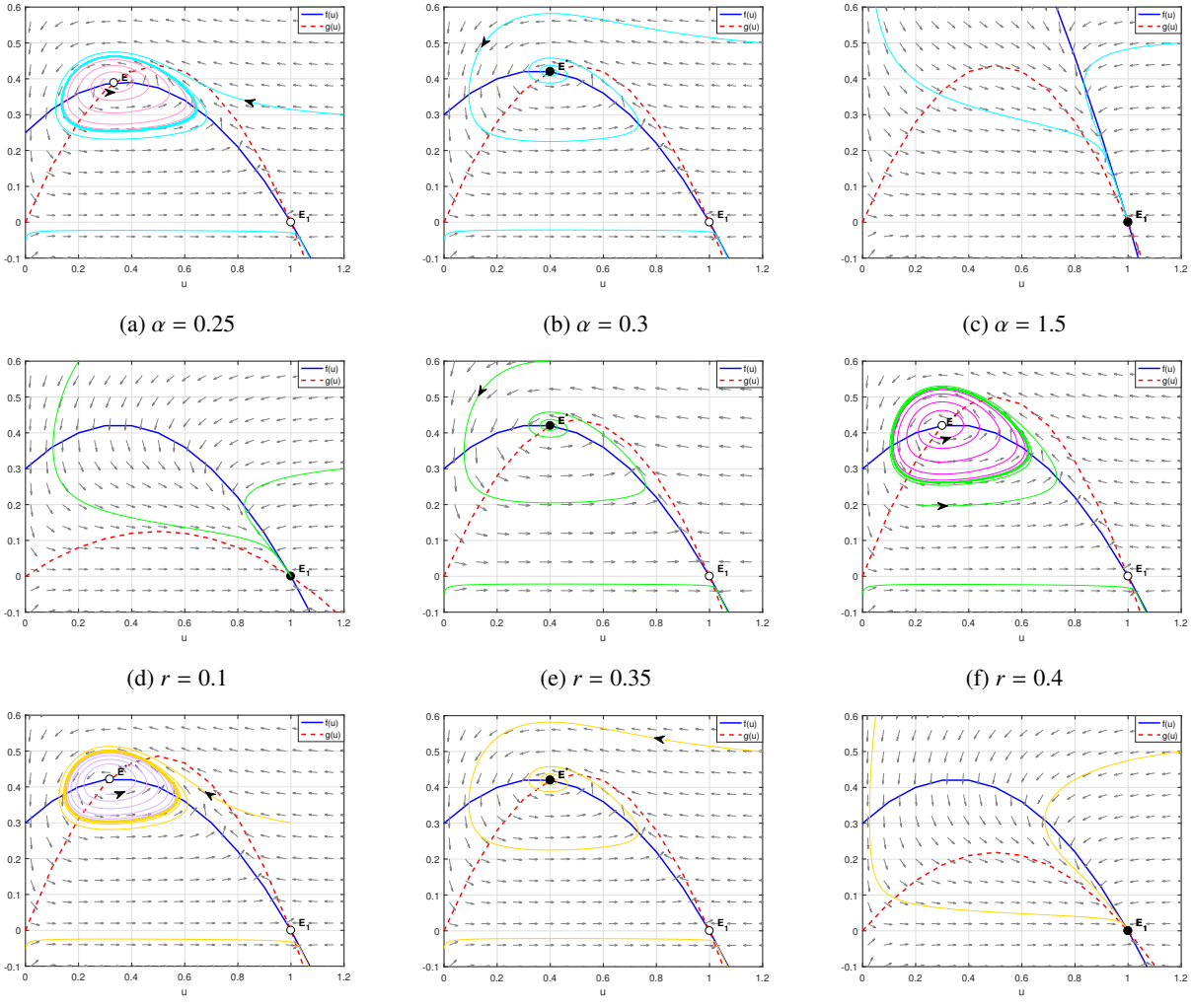

(a) $\alpha = 0.25$ (b) $\alpha = 0.3$ (c) $\alpha = 1.5$

(d) $r = 0.1$ (e) $r = 0.35$ (f) $r = 0.4$

(g) $\sigma = 0.18$ (h) $\sigma = 0.2$ (l) $\sigma = 0.4$

Figure 2. The dynamic processes of (a) to (l) corresponding to Figure 1. The blue solid curves and the red dashed curves represent isocline lines, where $f(u) = (1-u)(u+\alpha)$, $g(u) = \frac{ru(1-u)}{u+\alpha}$. The green (pink) solid curves indicate the trajectory.

4.2. Numerical simulation to the delay τ for system (1.3)

In this subsection, we mainly discuss the influence of time delay parameters τ on the dynamic behavior of the system (1.3). According to $\alpha = 0.3, r = 0.35, \sigma = 0.2$, we have $E^*(0.4, 0.42)$, and $a_{11} = -0.0571428571 < 0$, which can ensure that the positive equilibrium E^* of system (1.1) is locally asymptotically stable. Further, selecting $d_{11} = 0.02, d_{12} = 0.01, d_{21} = 0.011, d_{22} = 0.025$, we know $\Delta_0 = -0.00006456959183 < 0, \Delta_1 = 0.0001133732653 > 0$, which means that $b_k + c_k > 0$ and $b_k - c_k < 0$ are true simultaneously if $k \in [0, \sqrt{m_3})$ with $m_3 = 21.03183477$. (Here, $k \in \{0, 1, 2, 3, 4\}$ because k represents the wave number and should be integer.) Therefore, the condition of Theorem 2.2 is satisfied. Next, according to (2.9) and (2.10), the discrete graph of time delay varying with wave number $k \in \{0, 1, 2, 3, 4\}$ can be described as Figure 3. It is found that the critical delay is $\tau_c = \min\left\{\tau_k^{(j)}\right\} = \tau_0^{(0)} = 1.1228$.

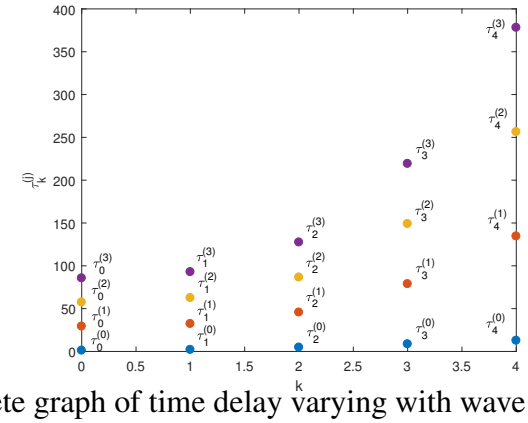

Figure 3. The discrete graph of time delay varying with wave number k, $k \in [0, \sqrt{m_3})$.

In order to further analyze the influence of parameters α, r, σ on τ_c, we use the statistical technique of partial rank correlation coefficients (PRCCs) to evaluate the strength and direction of the correlation between input parameters α, r, σ, and τ_c with PRCC values ranging from $[-1, 1]$. It is worth noting that parameters with higher absolute values of PRCC have a more significant impact on τ_c. Therefore, parameters that have a positive impact (through positive PRCC values) or a negative impact (through negative PRCC values) on τ_c can be identified. From Figure 4, it can be seen that parameters α and σ have a negative impact on τ_c, while parameter r has a positive impact. Based on Theorem 2.2 and sensitivity analysis, we can conclude that reducing parameters α and σ or directly increasing parameter r can increase the value of τ_c, resulting in a larger stable region for both predators and prey. Therefore, understanding the parameters and their specific effects on τ_c provides valuable insights for implementing targeted interventions or management measures.

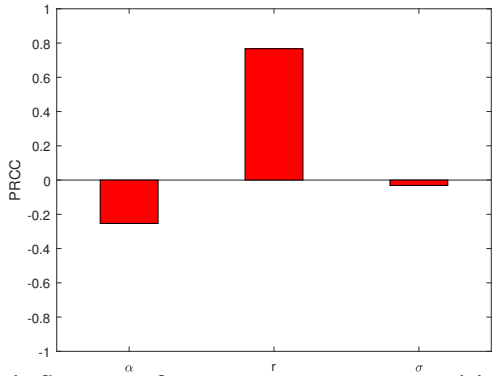

Figure 4. The influence of parameter α, r, σ on critical time delay τ_c.

4.3. *Hopf bifurcation of the delayed reaction-diffusion system* (1.3)

In this subsection, we mainly analyze the influence of the parameters τ on the Hopf bifurcation of the delayed reaction-diffusion system (1.3). Through simple calculations, we know $M = 0.007344156157 + 0.2213334635i$, $N = -0.12187341 + 0.9253030931i$. Thus, we know that the Hopf bifurcation of system (1.3) is a supercritical bifurcation according to Theorem 3.1.

As shown in Figure 5(a), when $\tau < \tau_c$, that is, $\tau_\varepsilon \approx \tau - \tau_c < 0$, the positive equilibrium E^* is always stable. When $\tau > \tau_c$, that is, $\tau_\varepsilon \approx \tau - \tau_c > 0$, the positive equilibrium E^* loses its stability, and a stable periodic solution appears. To more specifically study the effectiveness of the delay on oscillations, the time evolution diagrams of six time delays are presented in Figure 5(b). Obviously, with the increase of the τ, the amplitudes and periods of the prey oscillations increase significantly, which suggests that the amplitudes and periods of these oscillations are sensitive to the variation of τ.

In fact, taking $\tau = 0.8$, that is, $\tau_\varepsilon = -0.3228 < 0$, the system (1.3) eventually stabilizes at equilibrium E^* in Figure 6(a) under different boundary conditions. Next, considering $\tau = 1.5$, that is, $\tau_\varepsilon = 0.3772 > 0$, the periodic solutions of system (1.3) appear near the equilibrium E^*, as shown in Figure 6(b). In summary, when the transcription time delay is greater than zero and less than a certain value, the steady state is locally asymptotically stable. When the time delay exceeds a certain value, the steady state becomes unstable and exhibits periodic oscillations.

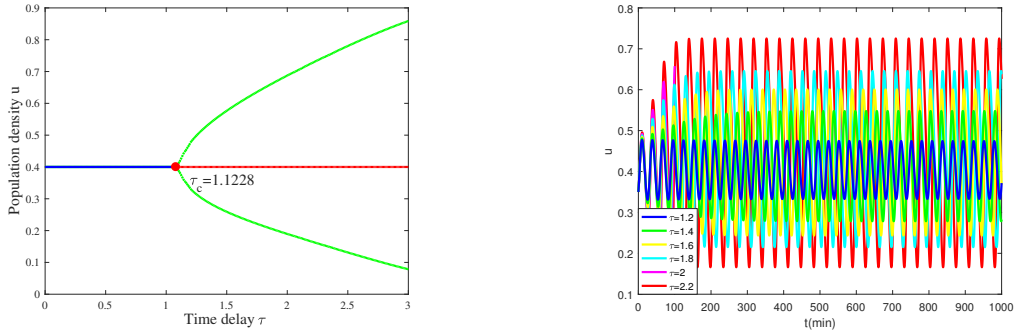

(a) (b)

Figure 5. (a) Hopf bifurcation diagrams of system (1.3) about τ. (b) The impact of the delay on amplitudes and periods of oscillations.

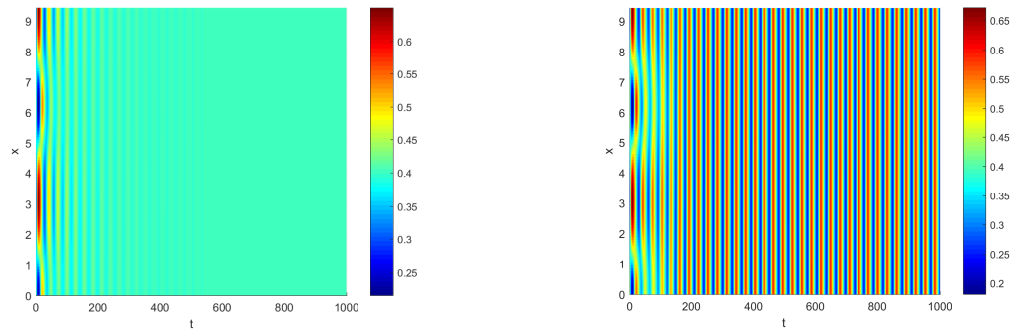

(a) (b)

Figure 6. The stability of the positive equilibrium E^* of system (1.3) with different τ. (a) $\tau = 0.8 < \tau_c$; (b) $\tau = 1.5 > \tau_c$. The color bar represents the value of $u(x, t)$. (a)(b) Inhomogeneous initial condition: $u(x, 0) = 0.35 + 0.1\cos(3\pi x)$, $v(x, 0) = 0.4 + 0.1\cos(3\pi x)$.

4.4. Numerical simulation of the Turing bifurcation of system (1.3)

In this section, we mainly focus on whether diffusion has an impact on the dynamic behavior of the system (1.3). Taking $\tau = 0.5 \in [0, \tau_c)$, $d_{11} = 0.02, d_{12} = 0.01, d_{21} = 0.011, d_{22} = 0.025$ and initial functions $(0.35 + 0.1\cos(3\pi x), 0.4 + 0.1\cos(3\pi x))$, the equilibrium E^* is locally asymptotically stable as shown in Figure 7(a). Next, we change $d_{11}, d_{12}, d_{21}, d_{22}$ separately, as shown in Table 1.

According to the Theorem 2.1 and Table 1, it is found that diffusion induces the emergence of Turing instability, as shown in Figure 7(b)–(e). Specifically, self-diffusion suppresses the occurrence of Turing instability, which indicates that when the population density of a region temporarily increases due to fluctuations, individuals tend to spread from high-density areas to low-density areas, rapidly reducing this density difference and restoring the population to a state of uniform distribution. This maintains the spatial stability of the system and prevents excessive aggregation or collapse of local populations.

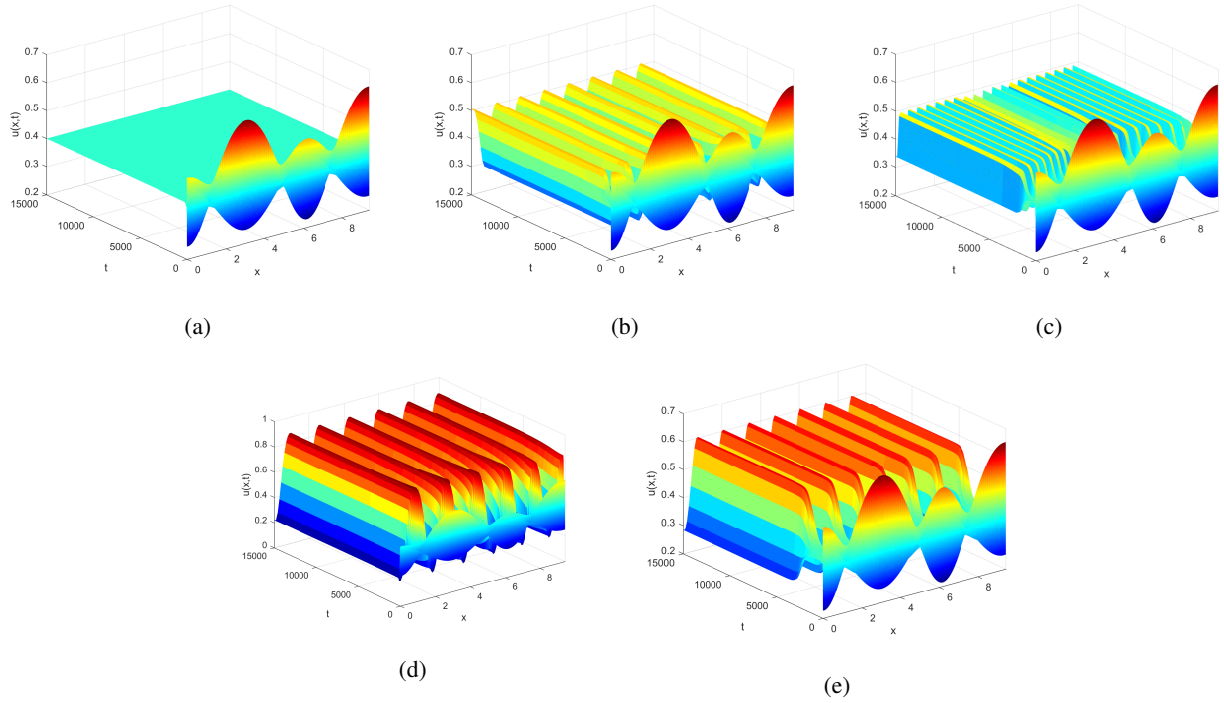

Figure 7. Turing instability induced by diffusion. (a) The standard parameter values are $d_{11} = 0.02, d_{12} = 0.01, d_{21} = 0.011, d_{22} = 0.025$; (b) $d_{11} = 0.007$; (c) $d_{12} = 0.0453$; (d) $d_{21} = 0.022$; (e) $d_{22} = 0.0108$.

Table 1. Diffusion coefficient and Turing instability condition.

d_{11}	d_{12}	d_{21}	d_{22}	Δ_0	ρ_2	Figure
0.07	0.01	0.011	0.025	$2.28755102 \times 10^{-6}$	-0.003957142857	(b)
0.02	0.04534	0.011	0.025	$3.438188088 \times 10^{-7}$	-0.000776542857	(c)
0.02	0.01	0.022	0.025	$4.73161224 \times 10^{-5}$	-0.01024285714	(d)
0.02	0.01	0.011	0.0108	9.3355918×10^{-7}	-0.004768571428	(e)

While cross-diffusion promotes the occurrence of Turing instability, the movement driven by the

interaction between predators and prey can trigger and amplify small spatial random fluctuations, ultimately forming a stable spatial pattern.

In short, the complex spatial patterns observed in ecosystems are not always driven by environmental heterogeneity, such as topography and resource distribution. It can be spontaneously generated through the cross-diffusion mechanism of behavioral responses (chasing and dodging) between individual organisms. The spatial structure generated by biological interactions itself is of crucial importance for the long-term coexistence of populations, the maintenance of biodiversity, and the stability of ecosystems.

5. Conclusions

In this paper, we investigate a predator-prey system with time delay, and self and cross diffusion. Initially, the existence and local stability of two boundary equilibria and a coexistence equilibrium of system (1.3) without time delay and diffusion are analyzed. Subsequently, we utilize multi-scale analysis near the Hopf bifurcation curve to investigate the effect of time delay on the system (1.3). Finally, the correctness of the theoretical results is verified through numerical simulations, and some interesting phenomena are revealed.

Time delay is an important parameter for studying Hopf bifurcation and is necessary for the oscillatory behavior of the predator-prey system. When the time delay is less than the critical time delay, the two populations will tend to the density value of the coexisting equilibrium. When the delay exceeds the critical time delay, the topological structure of the coexisting equilibrium changes, that is, it loses its stability through Hopf bifurcation and produces periodic oscillations. Next, we further investigate the direction of Hopf bifurcation at the coexistence equilibrium and the stability of periodic solutions by using the normal form theory. In multiple population dynamics systems, periodic oscillations may have dual ecological significance: positive aspects, such as promoting population learning of new survival strategies or triggering adaptive physiological changes, and negative aspects, such as inducing population variation or exacerbating environmental risks. Therefore, the generation and evolution of periodic behavior become an important issue when studying inter-species or intra-species relationships. Finally, we investigate the impact of diffusion on system dynamics, and find that self-diffusion suppresses the occurrence of Turing instability, while cross-diffusion promotes the occurrence of Turing instability. The movement behavior of organisms tends to maintain a uniform distribution of populations and stabilize ecosystems. The movement of organisms due to interactions such as avoidance or search will drive the formation of spatial heterogeneity patterns, thereby reshaping the structure of ecosystems.

Based on some research findings in this paper, we can consider high-dimensional bifurcation phenomena, such as Turing-Hopf bifurcation [22], Bogdanov-Takens bifurcation, double Hopf bifurcation, etc. Random phenomena are very common in life sciences; therefore, adding random factors to the predator-prey system in this paper and studying random phenomena is a hot topic. All of this will become our future research work.

Author contributions

Ping Li: Writing original draft, Visualization, Formal analysis, Software; Haisong Cao: Editing and writing review, Funding acquisition; Can Chen: Reviewing the paper, Funding acquisition; and

Jianfeng Jiao: Methodology, Conceptualization, Funding acquisition, Investigation, Supervision.

Use of Generative-AI tools declaration

The authors declare they have not used Artificial Intelligence (AI) tools in the creation of this article.

Acknowledgments

This work was supported by the National Natural Science Foundation of China (12401655), Natural Science Foundation of Henan Province (252300420350), the Project of Youth Backbone Teachers of Colleges and Universities in Henan Province (2023GGJS112), Basic Research Projects of Key Scientific Research Projects Plan in Henan Higher Education Institutions (242X008, 252X013). Key scientific research projects of Henan Institutions of Higher learning (24B110007), the Postgraduate Education Reform and Quality Improvement Project of Henan Province (YJS2025KC03, YJS2026AL002).

Conflict of interest

The authors declare that they have no known competing financial interests or personal relationships that could have appeared to influence the work reported in this paper.

References

1. B. Blasius, L. Rudolf, G. Weithoff, U. Gaedke, G. Fussmann, Long-term cyclic persistence in an experimental predator-prey system, *Nature*, **577** (2020), 226–230. https://doi.org/10.1038/s41586-019-1857-0
2. F. R. Zhang, Y. Li, C. P. Li, Hopf bifurcation in a delayed diffusive leslie-gower predator-prey model with herd behavior, *Int. J. Bifurcat. Chaos*, **29** (2019), 1950055. https://doi.org/10.1142/S021812741950055X
3. M. Song, S. Gao, C. Liu, Y. Bai, L. Zhang, B. Xie, et al., Cross-diffusion induced Turing patterns on multiplex networks of a predator-prey model, *Chaos Soliton. Fract.*, **168** (2023), 113131. https://doi.org/10.1016/j.chaos.2023.113131
4. A. J. Lotka, Analytical note on certain rhythmic relations in organic systems, *Proc. Natl. Acad. Sci. U.S.A.*, **6** (1920), 410–415. https://doi.org/10.1073/pnas.6.7.410
5. V. Volterra, Fluctuations in the abundance of a species considered mathematically[1], *Nature*, **118** (1926), 558–560. https://doi.org/10.1038/118558a0
6. C. S. Holling, The functional response of predators to prey density and its role in mimicry and population regulation, *Memoirs of the Entomological Society of Canada*, **97** (1965), 5–60. https://doi.org/10.4039/entm9745fv
7. C. S. Holling, Some characteristics of simple types of predation and parasitism, *Can. Entomol.*, **91** (1959), 385–398. https://doi.org/10.4039/ent91385-7
8. F. Wu, Y. J. Jiao, Stability and Hopf bifurcation of a predator-prey model, *Bound. Value Probl.*, **2019** (2019), 129. https://doi.org/10.1186/s13661-019-1242-9

9. C. Wang, S. Yuan, H. Wang, Spatiotemporal patterns of a diffusive prey-predator model with spatial memory and pregnancy period in an intimidatory environment, *J. Math. Biol.*, **84** (2022), 12. https://doi.org/10.1007/s00285-022-01716-4

10. R. J. Han, B. X. Dai, Spatiotemporal pattern formation and selection induced by nonlinear cross-diffusion in a toxic-phytoplankton-zooplankton model with Allee effect, *Nonlinear Anal.-Real*, **45** (2019), 822–853. https://doi.org/10.1016/j.nonrwa.2018.05.018

11. X. Y. Meng, L. Xiao, Hopf bifurcation and Turing instability of a delayed diffusive Zooplankton-Phytoplankton model with hunting cooperation, *Int. J. Bifurcat. Chaos*, **34** (2024), 2540090. https://doi.org/10.1142/S0218127424500901

12. X. Tao, L. Zhu, Study of periodic diffusion and time delay induced spatiotemporal patterns in a predator-prey system, *Chaos Soliton. Fract.*, **150** (2021), 111101. https://doi.org/10.1016/j.chaos.2021.111101

13. Z. W. Liang, X. Y. Meng, Stability and Hopf bifurcation of a multiple delayed predator-prey system with fear effect, prey refuge and Crowley-Martin function, *Chaos Soliton. Fract.*, **175** (2023), 113955. https://doi.org/10.1016/j.chaos.2023.113955

14. G. Sun, Z. Jin, L. Li, M. Haque, B. Li, Spatial patterns of a predator-prey model with cross diffusion, *Nonlinear Dyn.*, **69** (2012), 1631–1638. https://doi.org/10.1007/s11071-012-0374-6

15. G. Sun, Z. Jin, Y. Zhao, Q. Liu, L. Li, Spatial pattern in a predator-prey system with both self- and cross-diffusion, *Int. J. Mod. Phys. C*, **20** (2009), 71–84. https://doi.org/10.1142/S0129183109013467

16. H. Yang, Z. M. Zhong, Turing instability of the periodic solutions for a predator-prey model with Allee effect and cross-diffusion, *Adv. Cont. Discr. Mod.*, **2025** (2025), 53. https://doi.org/10.1186/s13662-025-03893-0

17. C. Y. Wang, S. Y. Qi, Spatial dynamics of a predator-prey system with cross diffusion, *Chaos Soliton. Fract.*, **107** (2018), 55–60. https://doi.org/10.1016/j.chaos.2017.12.020

18. D. X. Song, Y. L. Song, C. Li, Stability and Turing patterns in a predator-prey model with hunting cooperation and Allee effect in prey population, *Int. J. Bifurcat. Chaos*, **30** (2020), 2050137. https://doi.org/10.1142/S0218127420501370

19. Y. H. Peng, H. Y. Ling, Pattern formation in a ratio-dependent predator-prey model with cross-diffusion, *Appl. Math. Comput.*, **331** (2018), 307–318. https://doi.org/10.1016/j.amc.2018.03.033

20. D. X. Jia, T. H. Zhang, S. L. Yuan, Pattern dynamics of a diffusive toxin producing phytoplankton-zooplankton model with three-dimensional patch, *Int. J. Bifurcat. Chaos*, **29** (2019), 1930011. https://doi.org/10.1142/S0218127419300118

21. X. Z. Lian, S. L. Yan, H. L. Wang, Pattern formation in predator-prey model with delay and cross diffusion, *Abstr. Appl. Anal.*, **2013** (2013), 147232. https://doi.org/10.1155/2013/147232

22. W. J. Li, L. T. Zhang, J. D. Cao, A note on Turing-Hopf bifurcation in a diffusive Leslie-Gower model with weak Allee effect on prey and fear effect on predator, *Appl. Math. Lett.*, **172** (2026), 109741. https://doi.org/10.1016/j.am1.2025.109741

Appendix

The delay term in (3.2) is $v(x,t-1) = v(x,T_0-1,T_1-\varepsilon,T_2-\varepsilon^2,...)$. The Taylor expansion of $v(x,t-1)$ at $v(x,T_0-1,T_1,T_2,...)$ is as follows:

$$\begin{aligned}
&v(x,t-1)\\
=&v(x,T_0-1,T_1-\varepsilon,T_2-\varepsilon^2,...)\\
=&\varepsilon v_1(x,T_0-1,T_1-\varepsilon,T_2-\varepsilon^2,...)+\varepsilon^2 v_2(x,T_0-1,T_1-\varepsilon,T_2-\varepsilon^2,...)\\
&+\varepsilon^3 v_3(x,T_0-1,T_1-\varepsilon,T_2-\varepsilon^2,...)+...\\
=&\varepsilon\Big(v_1(x,T_0-1,T_1,T_2,...)-\varepsilon D_1 v_1(x,T_0-1,T_1,T_2,...)\\
&-\varepsilon^2 D_2 v_1(x,T_0-1,T_1,T_2,...)+...\Big)+\varepsilon^2\Big(v_2(x,T_0-1,T_1,T_2,...)\\
&-\varepsilon D_1 v_2(x,T_0-1,T_1,T_2,...)+...\Big)+\varepsilon^3 v_3(x,T_0-1,T_1,T_2,...)+...\\
=&\varepsilon v_{1,1}+\varepsilon^2(v_{2,1}-D_1 v_{1,1})+\varepsilon^3(v_{3,1}-D_1 v_{2,1}-D_2 v_{1,1})+...,
\end{aligned}$$

where $v_{m,1} = v_m(x,T_0-1,T_1,T_2,...)$.